

1 **Source analyses of axial and vestibular evoked potentials associated with brainstem-**
2 **spinal reflexes show cerebellar and cortical contributions.**

3
4
5 4 Neil PM Todd^{1,2}, Sendhil Govender^{2,3} Louis Lemieux⁴ and James G Colebatch^{2,3}
6
7 5

8
9 6 ¹Department of Psychology,
10 University of Exeter, Exeter EX4 4QC, UK;
11 7

12 ²Prince of Wales Clinical School and
13 8

14 ³Neuroscience Research Australia
15 9
16 10 UNSW, Sydney, NSW 2052, Australia;
17

18 11 and
19

20 12 ⁴UCL Queen Square Institute of Neurology, University College London, Queen Square,
21 London WC1N 3BG, UK.
22 13
23
24 14
25 15
26

27 16 Corresponding author:
28

29 17 Neil Todd
30

31 18 Email: n.todd@exeter.ac.uk
32
33 19
34 20
35
36 21
37
38 22
39
40 23
41
42 24
43
44 25
45

46 26 **Highlights:**
47 27
48

- 49 28 • Short latency potentials were evoked over the posterior fossa with vestibular and axial
50 stimuli
51 29
52 30 • Source analysis showed potentials arose predominantly from within the cerebellum and
53 medial forebrain
54 31
55 32 • Cerebellar excitability changes preceded soleus EMG by approximately 45 ms
56
57 33 • Medial forebrain activations may facilitate subsequent voluntary responses
58
59
60
61
62
63
64
65

34 **ABSTRACT**

1
2 35 In this work we examine the possible neural basis for two brainstem-spinal reflexes
3
4 36 using source analyses of brain activity recorded over the cortex and posterior fossa. In a
5
6 37 sample of 5 healthy adult subjects, using axial and vestibular stimulation by means of applied
7
8 38 impulsive forces, evoked potentials were recorded with 63 channels using a 10% cerebellar
9
10 39 extension montage. In parallel, EMG was recorded from soleus and tibialis anterior muscles
11
12 40 and accelerometry from the lower leg. Recordings over the cerebellum (ECeG) confirmed the
13
14 41 presence of short latency (SL) potentials and these were associated with changes in high-
15
16 42 frequency power. The SL responses to the two stimulus modalities differed in that the axial
17
18 43 stimulation produced an initial pause and then a burst in the high-frequency ECeG, followed
19
20 44 by excitation/inhibition in soleus while vestibular stimulation produced an initial burst then a
21
22 45 pause, followed by inhibition/excitation in soleus. These short latency responses were
23
24 46 followed by longer latency N1/P2/N2 responses in the averaged EEG, which were maximal at
25
26 47 FCz. Brain Electrical Source Analysis (BESA) demonstrated both cerebellar and cerebral
27
28 48 cortical contributions to the short-latency responses and primarily frontal cortex contributions
29
30 49 to the long-latency EPs. The latency and polarity of the SL EPs, in conjunction with changes
31
32 50 in high-frequency spontaneous activity, are consistent with cerebellar involvement in the
33
34 51 control of brainstem-spinal reflexes. The early involvement of frontal cortex and subsequent
35
36 52 later activity may be an indicator of the activation of the cortical motor-related system for
37
38 53 rapid responses which may follow the reflexive components. These findings provide evidence
39
40 54 of the feasibility of non-invasive electrophysiology of the human cerebellum and have
41
42 55 demonstrated cerebellar and frontal activations associated with postural-related stimuli.
43
44
45
46
47
48
49
50
51
52
53
54
55
56
57

58 1. INTRODUCTION

59 Knowledge of the electrophysiology of the human cerebellum is very limited, despite
60 its potential importance. The cerebellum has its own intrinsic rhythms (electrocerebellogram,
61 ECEG) which have a higher frequency content than cortical EEG [1-2]. Delal et al. [3]
62 summarised the limited observations available on the human electrocerebellogram, noting
63 “the electrophysiology of the human cerebellum remains largely unexplored”. They point out
64 that the posterior cerebellar cortex is at a similar depth as the occipital cortex from which
65 EEG (and evoked potentials) are easily measured. Delal et al [3] were aware of only 2 scalp
66 EEG recordings of cerebellar activity. Reports of evoked responses are equally rare, despite
67 there being clear evidence of short latency afferent input from the limbs [4]. There is one
68 report using evoked responses from over the cerebellum during intraoperative monitoring [5].
69 These authors reported a small N33-P40 response to tibial nerve stimulation with recordings
70 made over the posterior scalp with similar waveforms from electrodes placed over the
71 cerebellum.

72 We have investigated central vestibular projections by means of evoked potentials.
73 We have used the same acoustic and inertial activations of the vestibular end-organs that
74 produce vestibular evoked myogenic potentials (VEMPs), which in turn are manifestations of
75 vestibular reflex pathways. Using high-density EEG recordings and applying brain electrical
76 source analysis (BESA) methods, we have been able to show the origins of these potentials
77 include cerebellar sources [6-8]. Most recently using the above methods, we provided
78 evidence that short-latency (SL) potentials of likely cerebellar origin co-occur with the
79 VEMPs [9], hence we use the term vestibular cerebellar evoked potentials (or VsCEPs). In
80 the course of this work, we also discovered that it is possible to record the spontaneous
81 activity of the cerebellum, the ECEG [10], which like VsCEPs can be modulated by stimulus
82 input and context. Both VsCEPs and the ECEG show plasticity and context dependency,
83 typical characteristics of the cerebellum and learning and adaptive timing mechanisms [11].

84 In the present article we have investigated VsCEPs and the ECEG in combination with
85 a novel extension of the 10-10 electrode placement system over the posterior fossa. Our aim
86 was to provide further detail and resolution on the nature of cerebellar evoked potentials
87 (CEPs) associated with postural reflexes. We were interested to explore the possibility of
88 recording CEPs associated with another putative brainstem-dependent postural reflex, in
89 addition to those produced by vestibular activation. We, therefore, also investigated CEPs
90 produced by axial acceleration which has been established to produce well-defined SL spinal
91 reflexes. This reflex is hypothesized to be mediated through the brainstem and to descend

92 through the reticulo-spinal system [7-9]. Preliminary investigations suggested this stimulus
93 too was associated with a clear SL CEP. Our principal approach was the use of source
94 analysis of the EEG/ECeG with the aim of comparing the sites of generation within the
95 cerebellum. In conjunction with this we undertook a spectral power analysis of the ECeG.

97 **2. MATERIALS AND METHODS**

98 **2.1 Subjects**

99 Five adult healthy subjects (4 males and 1 female) were recruited from staff at the
100 Prince of Wales Hospital and Western Sydney University. All subjects gave written informed
101 consent before experimentation and the study was approved by the local ethics committee.
102 The work described has been carried out in accordance with the Declaration of Helsinki.

104 **2.2 Stimuli**

105 Vestibular and axial stimuli were delivered using a hand-held mini-shaker (model
106 4810, Brüel & Kjaer P/L, Denmark) with an acrylic rod attached. The stimulus waveform
107 was a 3rd order gamma function with a 4 ms rise time [15], chosen as an impulsive waveform
108 with a smooth onset. Customized software was used to generate the waveform using a
109 Power1401 (CED, UK) and fed to a power amplifier (model 2718, Brüel & Kjaer P/L,
110 Denmark). The intensity was 20 V peak, equivalent to approximately 14N peak force level
111 (FL). For the vestibular stimulus, the mini-shaker was applied to the left mastoid of all
112 subjects using a positive phase polarity (i.e. initial movement of the acrylic rod was towards
113 the head). This has shown to be an effective vestibular stimulus, capable of evoking postural
114 responses in the legs [16,17]. For the axial stimulus the mini-shaker was applied to the
115 spinous process of the C7 vertebra during anterior lean [13].

117 **2.3 EEG/ECeG recording**

118 63 channels of EEG/ECeG were recorded from over the scalp and neck using a novel
119 10% cerebellar-extended 10-10 system cap (made to our custom design by EASYCAP
120 GmbH, Germany). The cerebellar extension was designed by completing the population of
121 the Iz row, labelled using the standard nomenclature, from P9 to P10, and adding two
122 additional 10% rows inferiorly, from P11 to P12 and from P13 to P14. Subsequent to the cap
123 design, Heine et al. [18] published an extended electrode placement nomenclature which we
124 have adopted here. The electrodes were of Ag/AgCl type and maintained at 10 kOhms or
125 less. A ground electrode was placed at AFz with reference at Nz. Signals were amplified

126 using a combination of amplifiers, a 32-channel ActiChamp and a 32-channel Digitimer
127 D360/D120 (Digitimer Co, UK), filtered at 0.5 Hz to 3 kHz and sampled at 10 kHz. The 32
128 ActiChamp channels were recorded using BrainVision software (version 1.22, Brain Products
129 GmbH, Germany) and the 32 Digitimer amplified channels were sampled using a CED power
130 1401 and recorded using Signal software (version 6.02, Cambridge Electronic Design, UK).
131 Evoked potential peaks were named based upon their polarity and latency.

132 133 **2.4 EMG and accelerometry recording.**

134 In parallel with the EEG/ECeG, EMG recordings were made using adhesive
135 electrodes (Cleartrace 1700-030, Conmed Corp., USA) placed bilaterally over the soleus and
136 tibialis anterior (TA) muscles. Active electrodes were positioned 1-2 cm above the musculo-
137 tendinous junction for soleus and 1-2 cm lateral to the tibia for TA with reference electrodes
138 3 cm below the active electrodes. A ground electrode was placed on the right lower leg. EMG
139 signals were amplified (x1000, Medelec AA6 Mark III), band-pass filtered (8 Hz – 1.6 kHz),
140 sampled at 10 kHz using a Micro1401 (CED, UK) and recorded using the Signal software.
141 Uniaxial accelerometers (model 751-100, Endevco, USA) were placed over the tibial
142 tuberosities.

143 144 **2.5 Experimental procedure**

145 Recordings were made using two stimulus modalities under three timing conditions.
146 We plan to report the effects of timing conditions separately. Recording began 100 ms prior
147 to the first stimulus. The conditions were: *an irregular condition*, in which the stimuli were
148 presented with a random inter-trial interval (800 ms to 1400 ms), with a recording epoch of
149 700 ms; secondly, *a regular condition*, in which the stimuli were presented in the form of an
150 anapaest (“Three blind mice”) rhythm, with inter stimulus intervals of 600 ms and 1200 ms
151 (inter-trial interval 2400 ms) and, thirdly, *an uncertain condition*, where the third beat of the
152 anapaest rhythm was randomly absent on 50% of trials. The second and third conditions used
153 a longer recording epoch of 2100 ms. The stimulus modalities and timing conditions were
154 scheduled pseudo-randomly. The recordings took place with the subjects standing; for the
155 axial stimulation they were asked to lean forward, but look towards the horizon. Between
156 recordings subjects were allowed to rest sitting down. For the irregular condition subjects
157 were asked to count the total number of trials (75 - 80), for the regular condition to count the
158 number of times they heard “Three blind mice” (36 - 40) and for the uncertain condition to
159 count the number of times they heard the complete “Three blind mice” (46-50). Subjects

160 were asked to report the number and this was recorded for the purpose of ensuring that they
161 were attending to the stimuli.

162 The timing of the trials, stimulus delivery and synchronisation of the parallel EEG and
163 EMG recording systems was controlled by custom software driving a second Power1401
164 digital output. The triggers for the stimuli (either one, two or three per trial) were generated
165 from digital outputs with Signal software while recording the 32 EEG channels. Markers for
166 epoch zero point and trial type were also recorded.

168 **2.6 Data analysis**

169 After recording EEG/ECeG we performed source localization using the whole 63
170 channels, spectral power analyses of selected channels followed by analysis of the EMG and
171 accelerometry recordings.

173 *2.6.1 EEG/ECeG*

174 All EEG/ECeG recordings were screened for blinks and other artefacts (about 5 –
175 10% trials) and then merged together using the Scan software (version 4.5, Compumedics
176 Ltd, Australia) and BESA software (version 6.1, MEGIS Software GmbH, Germany). For the
177 electrical source analysis the data were averaged across all timing conditions.

179 *2.6.2 Brain Electrical Source Analyses (BESA)*

180 The standard four-shell ellipsoidal head model was employed with radial thicknesses
181 of 85, 6, 7 and 1 mm for respectively the head, scalp, bone and CSF, with conductivities of
182 0.33, 0.33, 0.0042 and 1.0, respectively. The fitting was carried out using the BESA genetic
183 algorithm with standard parameter settings.

184 A modelling strategy was adopted to run each genetic algorithm fit 10 times to test its
185 reproducibility using different starting points. A series of models increasing complexity,
186 from one up to 10 dipoles, was run on the short latency epoch (7 – 74 ms) for the two
187 modalities, and then again over the whole epoch (7 – 500 ms) for comparison. For the
188 vestibular condition with four sources the cerebellar sources were constrained to be
189 symmetrical, based on our previous report [19]. For the low order models (up to 4 dipoles)
190 the solutions were unique, but for higher order models, the number of differing solutions
191 increased, indicating that there were likely to be a number of smaller contributors to the
192 recorded surface potentials, in addition to the major sources. Here we have used 4- and 10-
193 dipole model solutions (the latter the maximum allowed on degrees of freedom constraints

194 for 63 channels with 6 degrees of freedom per dipole). For the 10-dipole model, run 10
195 times, the resultant 100 locations were then subject to a hierarchical cluster analysis, using
196 the between-groups linkage method with squared Euclidian distance measure, in order to
197 eliminate the non-viable and very weak sources. The 10 runs were repeated for both the short
198 and whole epochs for both stimulus modalities, giving a total of 400 dipole locations. A 5
199 mm³ standard deviation was imposed on the cluster volumes and any isolated single dipole
200 sources which resulted from that constraint were eliminated. In addition to the mean
201 Talairach-Tournoux coordinates of the final surviving clusters, a weight was attributed to the
202 clusters derived from the number of dipoles making up the cluster divided by 10 (runs). Thus
203 if the same source appeared for every run its weight would be 1.0.

204 For cerebellar coordinates the Schmahmann et al. [20] atlas was used to determine the
205 anatomical locations, while for other locations the Talairach Client application (talairach.org,
206 version 2.4.3) was employed with a +/- 5mm³ search.

208 *2.6.3 Spectral power analyses of spontaneous cerebellar activity*

209 In order to measure any high-frequency pausing or bursting, characteristic of post-
210 climbing fibre responses, a spectral power analysis was also conducted on electrode sites at
211 which the CEPs were most clearly recorded on the scalp (Iz for the axial, PO10 for the
212 vestibular). This used the continuous wavelet transform (CWT) as implemented in the
213 MATLAB toolbox (R2019b, Mathworks, Natick, CA). In the present analysis a Morlet
214 wavelet was employed at a density of 24 voices per octave over 9 octaves. In order to ensure
215 conservation of energy a correction of factor $\sqrt{\frac{10}{f}}$ was applied to match the Fourier equivalent.
216 The CWTs were further transformed to scaleograms (time-frequency images) from the
217 absolute value of the CWT and rescaled to be in dB per Hz re 1 μV^2 . Scaleograms were
218 computed for all trials, then further split into six frequency bands; alpha (α : 7.5-12.5 Hz),
219 beta (β : 13-30 Hz), gamma (γ : 30-80 Hz), ultra-gamma (u- γ : 80-160 Hz), very high frequency
220 (VHF: 160-320 Hz) and ultra-high frequency (UHF: 320-640 Hz). These were then averaged
221 to create a grand mean with 700 ms epoch. We also extracted the VHF power at the PO10
222 (vestibular stimulation) and Iz (axial) electrodes by digital filtering and then RMS (root mean
223 square) averaging. We measured the size of the burst and following pause to correlate these
224 changes with the initial EMG changes in soleus. Burst and pause activity were normalised to
225 the baseline.

227 *2.6.4 EMG/Accelerometry*

228 For each subject and timing condition, averaged RMS recordings of EMG and EEG
229 were used to quantify the evoked reflexes. Acceleration measurements were made for the
230 onset latency and the initial peak for amplitude. For the EMG and accelerometry data, an
231 ANOVA was conducted using modality (vestibular versus axial stimulation), condition
232 (irregular, regular and uncertain) and side (right and left) as factors. Pearson's correlations
233 were used to compare evoked neural responses and soleus EMG for amplitude, with $P < 0.01$
234 used as the threshold of significance due to the number of comparisons. EMG amplitudes
235 were normalised to the baseline.

237 **3. RESULTS**

238 **3.1 Grand means of EEG/ECeG**

240 FIGURES 1 AND 2 HERE

242 Figures 1 and 2 show the CEP grand means for the axial and vestibular stimuli
243 respectively. Axial stimulation produced a complex sequence of SL waves consisting of
244 P13/N19/P25/N32/P50/N62 peaks at Iz (inverted at Bz). This sequence of waves was mostly
245 sagittally oriented (Figure 1B). For the vestibular case, SL waves consisted of P12/N17
246 peaks best observed at PO10, contralateral to the side of stimulation, consistent with previous
247 observations [19]. The potential maps showed this dipole was strongly lateralized (Figure
248 2B). We also identified additional SL waves for the vestibular case, N25/P40/N53 peaks,
249 which were prominent at Bz. In both cases, long-latency (LL) waves were present over
250 frontal electrodes, most prominently at FCz, which we label N1/P2/N2 by analogy to the
251 auditory LL potentials.

253 **3.2 Latencies and amplitudes of the SL and LL EPs.**

255 TABLE I HERE

257 Table 1 provides mean amplitude and latencies of the early SL EPs (recorded over the
258 posterior scalp) versus LL EPs (recorded at FCz) for the three timing conditions, averaged
259 across trials and for both modalities. For the first two SL waves (axial P13/N19 vs vestibular
260 P12/N17), an ANOVA of the latencies (Table II) indicated only the expected main effect of

261 “wave”. There was a tendency for earlier vestibular wave peaks than their axial counterparts
262 (by about 0.5 ms and 1.8 ms respectively) but this did not reach statistical significance. For
263 the SL amplitudes there was no main effect of wave but there was a main effect of
264 “modality”, with the vestibular amplitudes being significantly larger than for the axial
265 stimulus. There was also a two-way interaction between “wave” and “modality”: whereas for
266 the axial stimulus the second wave was dominant, for the vestibular case the first wave was
267 larger. Neither latencies nor amplitudes showed an effect of timing condition.

268
269 TABLE II HERE
270

271 When an ANOVA was carried out for the LL waves a different pattern emerged:
272 There were no significant effects of “modality” and, unlike the case for the SL waves, there
273 was an effect of timing condition on the amplitude. Specifically, lower amplitudes occurred
274 during the regular condition compared to the irregular and uncertain conditions. The
275 amplitudes and latencies both showed a main effect of “wave”, the P2 being larger than the
276 N1 and N2 and their having different latencies.

277 278 **3.3 Source analyses of the vestibular and axial grand means.**

279
280 FIGURE 3 HERE.
281

282 Figure 3 illustrates the structure of global field power for the grands means of the axial
283 (Figure 3A) and vestibular (Figure 3B) stimuli. Both modalities showed a series of short
284 latency lobes, which correspond to the waves identified above. These were followed by three
285 lobes of long latency corresponding to the LL waves N1/P2/N2, where for both stimuli the P2
286 lobe was dominant. A vertical line at 74 ms marks the approximate division between the short
287 and long epochs.

288
289 FIGURE 4 HERE
290

291 For the whole epoch, fitting up to four dipoles produced the same solution across the
292 repeated runs (i.e. four narrow clusters with weight = 1.0). Figure 4A & 4C illustrates the 4-
293 dipole solutions showing two cerebellar and two fronto-central sources for both modalities.
294 For the axial case (residual variance (RV) = 12%), the principal cerebellar source (Source 4:

295 Sc4) was close to the vermis in the posterior lobe. For the vestibular case (RV = 22%), the
296 cerebellar sources were more lateralised (and symmetrical, as imposed). The fronto-central
297 dipoles (Sc1 and Sc2) were similarly located in both modalities, indicating central and
298 anterior cingulate sources. Source currents (Figure 4B & 4D) showed that, for both
299 modalities, the cortical sources (Sc3 and Sc4) were strongly activated within the initial epoch
300 as well as during the later phase.

TABLES III AND IV HERE

304 For the 10-dipole model runs, the outcomes using hierarchical clustering are shown in
305 Tables III and IV. For the axial case, clustering resulted in 16 whole (w) and 15 short (s)
306 epoch clusters. For the vestibular case, clustering resulted in 15 whole (w) and 14 short (s)
307 epoch clusters. A notable difference between the effects of the two stimuli is the relative
308 contribution of cortical sources. For vestibular stimulation the cortical contribution was
309 largely confined to dorsal mid-line frontal sources. In contrast, for axial stimulation, the
310 cortical contribution was much more widespread, including ventral cingulate and prefrontal
311 cortex, along with parietal, temporal and occipital sources. Both modalities showed bilateral
312 cerebellar and brainstem activity. For axial stimulation, bilateral vermal lobules IX (tonsil)
313 were strongly activated, along with a more lateralised activation of H VIIB/crus II in the right
314 inferior semi-lunaris lobule. For vestibular stimulation, bilateral activation extended to H
315 VIIIA/B of the dorsal paraflocculus. In addition, both stimuli produced sources located
316 outside the brain – from around the eyes and right neck for vestibular simulation, and
317 bilateral neck for the axial stimulation. These were strongly weighted for the vestibular
318 stimulus and presumably represent VEMPs.

3.4 Spectral power of the cerebellar spontaneous activity and its relation to the evoked responses

FIGURE 5 HERE

324 Figure 5 shows scaleograms of spontaneous cerebellar activity (ECeG) for the two
325 modalities for the irregular timing condition. The power analysis indicated that axial
326 stimulation produced a different pattern of high-frequency pausing from the vestibular
327 stimulus (Fig 5A, B). The effects of axial stimulation consisted of an initial pause followed
328 by a prominent burst associated with the P50 (at Iz: Fig 5D). Vestibular stimulation (Fig 5G)

329 produced an initial burst of high-frequency power associated with the P12 wave at PO10 (Fig
330 5J) followed by pausing in the spontaneous activity, especially in the UHF and VHF bands
331 (Fig 5H). Illustrated for comparison are the four-dipole model cerebellar source 3 and 4
332 currents (Fig 5C, I).

336 3.5 EMG and accelerometry analyses

337 Figure 5 (E, K; F, L) illustrates the unrectified leg EMG and RMS averages, along
338 with leg acceleration. Overall, the evoked EMG response was larger for axial stimulation
339 ($F_{(1,44)} = 18.0$, $p < 0.001$). Axial stimulation also produced larger accelerations ($F_{(1,37)} = 60.1$,
340 $p < 0.001$, mean initial peak amplitudes: 6.4 ± 3.9 mg (axial) & 1.7 ± 0.8 mg (vestibular)) and
341 earlier responses ($F_{(2,74)} = 37.3$, $p < 0.001$, mean onset latencies: 5.6 ± 1.2 ms (axial) & $14.7 \pm$
342 2.7 ms (vestibular)).

343 The axial stimulus produced bilateral excitatory EMG responses with mean onset and
344 end times of 57.8 ± 3.2 ms and 80.7 ± 5.8 ms respectively, with a mean baseline-corrected
345 amplitude of $27.5 \pm 14.9\%$. In contrast, the vestibular stimulus produced an initially
346 inhibitory response beginning at 55.4 ± 5.8 ms and ending at 92.4 ± 4.4 ms with mean
347 amplitude of $12.3 \pm 8.7\%$. In both cases the EMG onset was preceded by CEPs and
348 associated changes in high-frequency activity. For vestibular stimulation the latency between
349 the onset of the large initial burst associated with the P12 potential and the onset of EMG
350 inhibition was about 48 ms. For axial stimulation, the latency between the onset of the
351 smaller initial pause associated with the P13, to the onset of EMG excitation was about 46
352 ms, while the latency between the onset of the axially-evoked P50 and associated burst and
353 the onset of EMG inhibition was about 44 ms.

354 For axial stimulation, the peak to peak P13-N19 amplitudes were significantly
355 correlated with the degree of excitation evoked in soleus ($r_{(26)} = 0.66$, $p < 0.001$). There was
356 no such correlation for the vestibular CEPs. For the vestibular stimulus, the size of the VHF
357 burst strongly correlated with the initial inhibitory change in soleus ($r_{(26)} = 0.64$, $p < 0.001$),
358 whereas for the axial stimulus there was a trend between the VHF pause and initial excitatory
359 change in soleus ($r_{(26)} = 0.34$, $p = 0.07$).

361 4. DISCUSSION

362 Our present findings confirm the value of recording over the posterior fossa and
1 363 below and this was made possible with the use of an extended EEG/ECeG cap. We found
2 364 short latency EPs in posterior electrodes which localised to the cerebellum followed by long-
3 365 latency EPs in fronto-central leads in response to two distinct stimulus modalities, axial and
4 366 vestibular. The findings for our vestibular stimulus confirm and extend our previous report of
5 367 vestibular-evoked cerebellar potentials [11,19,21]. The P12-N17 response in the present
6 368 study was maximal over PO10, which corresponds to Iz₊₆ in the Govender et al. [19] study.
7 369 Source analysis, both the 4- and 10-dipole models, showed strong sources bilaterally in the
8 370 cerebellum, principally in lobules VIIIA and VIIIB. Power analysis confirmed a pause in
9 371 background activity following the P12 potential, corresponding to the slow wave and this was
10 372 clearest for the UHF and VHF frequency bands. Source modelling also revealed additional
11 373 strong sources, for short and long latencies, within the cingulate gyrus, and activity was
12 374 shown at electrode FCz. The cortical/subcortical sources varied between the two stimuli with
13 375 the axial stimulus evoking more cortical foci, and both caused activation in the cerebellum.

376 Impulsive stimuli applied to the lower neck, “axial stimuli”, have been shown to
25 377 evoke postural reflexes. The afferent limb does not depend upon vestibular afferents [12,13]
26 378 and the reflex has been proposed to be a spino-bulbo-spinal one [22]. Like the vestibular
27 379 stimulus, the axial stimulus evoked robust regions of excitation within the cerebellum and the
28 380 medial forebrain. For the cerebellum, the most heavily weighted foci lay more medially and
29 381 were reflected in the recordings at Iz while FCz showed the frontal activations. In contrast to
30 382 the vestibular stimulus, the initial excitability changes for the ECEG were inhibitory rather
31 383 than excitatory. Both the vestibular and the axial stimuli are known to evoke postural
32 384 reflexes. For the vestibular stimulus, the effect on leg muscles is dependent upon head
33 385 orientation [23] and with the head straight, as here, only a small response in soleus would be
34 386 expected. In our case, responses were recorded in soleus which were initially excitatory for
35 387 the axial stimulus but inhibitory for the vestibular one. Corresponding to this and preceding
36 388 it by 43-45 ms, there were opposite changes in cerebellar excitability. The latency difference
37 389 is also consistent with previous observations of the likely descending conduction times
38 390 including the peripheral latency [22]. In the case of the axial stimulus, there was a correlation
39 391 between the size of the P13-N19 evoked response and the size of the following soleus EMG
40 392 excitation. For the vestibular stimulus, the VHF power changes showed a correlation
41 393 between the burst of cerebellar activity and the inhibition in soleus.

394 Previous studies investigating the effects of cerebellar disease on postural reflexes
58 395 have reported normal latencies but abnormalities in the scaling of responses, with larger and
59
60
61

396 more variable responses which fail to adapt in response to prior experience [24, 25].
397 Cerebellar cortical output is solely via Purkinje neurones which are purely inhibitory to their
398 cerebellar nuclear targets. The fastigial nucleus is the most important of these for posture and
399 projects to the medial reticular descending pathways [26, 27]. Eccles et al. [28] showed
400 monosynaptic input from fastigial nuclear neurons to reticulospinal neurones projecting to
401 both the upper and lower limbs. The effects of cerebellar disease and the excitability changes
402 we have found are both consistent with a modulatory role for cerebellar output on postural
403 reflexes and specifically on the brainstem-spinal postural reflexes that we have investigated
404 here.

405 The second major area of activation (sources 1 and 2, electrode FCz) was located on
406 the medial aspect of the hemispheres in the anterior and middle cingulate gyri. Watson et al.
407 [29] showed that electrical stimulation of the fastigial nucleus, the main output target for the
408 vermis and the nucleus most likely to be activated by our stimuli [27,30], evoked short
409 latency activation of perilimbic, M2 and cingulate areas. They speculated this input could
410 provide relevant proprioceptive information for higher order decision-making processes.
411 Here it may be relevant to note that the axial stimulus which we used needs only to be made
412 slightly stronger and longer in duration, for the reflex response to be followed by a powerful
413 and prolonged voluntary response required to remain upright [31]. The response on the
414 medial aspect of the hemispheres may have a role in mediating the rapid engagement of
415 voluntary pathways when required by a perturbation to stance.

416
417 **Acknowledgement:** This study was supported by the Prince of Wales Hospital Foundation.

418 **REFERENCES**

1
2 419

3
4 420 [1] E.D. Adrian, Discharge frequencies in the cerebral and cerebellar cortex, *J Physiol.* 83
5 421 (1935) 32P-33P. <https://doi.org/10.1111/tjp.1935.83.issue-suppl>.

6
7 422

8
9 423 [2] R.S Dow, The electrical activity of the cerebellum and its functional significance, *J.*
10 424 *Physiol.* 94 (1938) 67-86. <https://doi.org/10.1113/jphysiol.1938.sp003663>.

11
12 425

13
14 426 [3] S.S. Delal, D. Osipova, O. Bertrand, K. Jerbi, Oscillatory activity of the human
15 427 cerebellum: The intracranial electrocerebellogram revisited. *Neurosci. Biobehav. Rev.* 37
16 428 (2013) 585-593. <https://doi.org/10.1016/j.neubiorev.2013.02.006>.

17
18 429

19
20 430 [4] J.C. Eccles, L. Provini, P.Strata, H. Taborikova, Analysis of electrical potentials in the
21 431 cerebellar anterior lobe by stimulation of hindlimb and forelimb nerves, *Exp. Brain Res.* 6
22 432 (1968) 171-194. <https://doi.org/10.007/bf00235123>.

23
24 433

25 434 [5] R.J. Hurlbert, M.G. Fehlings, M.S. Moncada, Use of sensory-evoked potentials recorded
26 435 from the human occiput for intraoperative physiologic monitoring of the spinal cord. *Spine*
27 436 20 (1995) 2318-2327. <https://doi.org/10.1097/00007632-199511000-00010>.

28
29 437

30 438 [6] N.P.M. Todd, S.M. Rosengren, J.G. Colebatch, A source analysis of short-latency
31 439 vestibular evoked potentials produced by air- and bone-conducted sound, *Clin. Neurophysiol.*
32 440 119 (2008) 1881–1894. <https://doi.org/10.1016/j.clinph.2008.03.027>.

33
34 441

35 442 [7] N.P.M. Todd, A.C. Paillard, K. Kluk, E. Whittle, J.G. Colebatch, Source analysis of short
36 443 and long latency vestibular-evoked potentials (VsEPs) produced by left vs. right ear air-
37 444 conducted 500 Hz tone pips, *Hear. Res.* 312 (2014) 91–102.
38 445 <https://doi.org/10.1016/j.heares.2014.03.006>.

39
40 446

41 447 [8] N.P.M. Todd, S. Govender, J.G. Colebatch, Vestibular-dependent inter-stimulus interval
42 448 effects on sound evoked potentials of central origin, *Hear. Res.* 341 (2016) 190-201.
43 449 <https://doi.org/10.1016/j.heares.2016.07.017>.

44
45 450

- 451 [9] N.P.M. Todd, S. Govender, J.G. Colebatch, The inion response revisited: evidence for a
452 possible cerebellar contribution to vestibular-evoked potentials produced by air-conducted
453 sound stimulation, *J. Neurophysiol.* 117 (2017) 1000–1013.
454 <https://doi.org/10.1152/jn.00545.2016>.
- 455
456 [10] N.P.M. Todd, S. Govender, J.G. Colebatch, The human electrocerebellogram (ECeG)
457 recorded non-invasively using scalp electrodes, *Neurosci. Lett.* 682 (2018) 124–131.
458 <https://doi.org/10.1016/j.neulet.2018.06.012>
- 459
460 [11] N.P.M. Todd, S. Govender, J.G. Colebatch, Modulation of the human electro-
461 cerebellogram (ECeG) during vestibular and optokinetic stimulation, *Neurosci. Lett.* 712
462 (2019) 134497. <https://doi.org/10.1016/j.neulet.2019.134497>.
- 463
464 [12] K. Bötzel, P. Feise, O.I. Kolev, S. Krafczyk, T. Brandt, Postural reflexes evoked by
465 tapping forehead and chest, *Exp. Brain. Res.* 138 (2001) 446–451.
466 <https://doi.org/10.1007/s002210100726>.
- 467
468 [13] S. Graus, S. Govender, J.G. Colebatch, A postural reflex evoked by brief axial
469 accelerations, *Exp. Brain. Res.* 228 (2013) 73–85. [https://doi.org/10.1007/s00221-013-3539-](https://doi.org/10.1007/s00221-013-3539-8)
470 8.
- 471
472 [14] B. Teng, S. Govender, J.G. Colebatch, Postural responses in the upper limbs evoked by
473 axial impulses: a role for reticulospinal projections, *Exp. Brain. Res.* 235 (2017) 2235–2242.
474 <https://doi.org/10.1007/s00221-017-4963-y>.
- 475
476 [15] N.P.M. Todd, S.M. Rosengren, J.G. Colebatch, Ocular vestibular evoked myogenic
477 potentials (OVEMPs) produced by impulsive transmastoid accelerations, *Clin. Neurophysiol.*
478 119 (2008) 1638–1651. <https://doi.org/10.1016/j.clinph.2008.03.009>.
- 479
480 [16] R. Laube, S. Govender, J.G. Colebatch, Vestibular-dependent spinal reflexes evoked by
481 brief lateral accelerations of the heads of standing subjects, *J. Appl. Physiol.* 112 (2012)
482 1906–1914. <https://doi.org/10.1152/jappphysiol.00007.2012>.

- 484 [17] S. Govender, D.L. Dennis, J.G. Colebatch, Vestibular evoked myogenic potentials
1 485 evoked by air- and bone-conducted stimuli in vestibular neuritis, *Clin. Neurophysiol.* 126
2
3 486 (2015) 2004-2013. <https://doi.org/10.1016/j.clinph.2014.12.029>
4
5 487
6
7 488 [18] W. Heine, M.A. Dobrota, D. Schomer, R. Wigton, S. Herman, High-Density Adaptive
8
9 489 Ten Ten: Proposal for Electrode Nomenclature for High-Density EEG, *J. Clin. Neurophysiol.*
10
11 490 37 (2020) 263-270. <https://doi.org/10.1097/wnp.0000000000000632>.
12
13 491
14 492 [19] S. Govender, N.P.M. Todd, J.G. Colebatch, Mapping the vestibular cerebellar evoked
15
16 493 potential (VsCEP) following air- and bone-conducted vestibular stimulation, *Exp. Brain. Res.*
17
18 494 238 (2020) 601-620. <https://doi.org/10.1007/s00221-020-05733-x>.
19
20 495
21
22 496 [20] J.D. Schmahmann, J. Doyon, D. McDonald, C. Holmes, K. Lavoie, A.S. Hurwitz, N
23
24 497 Kabani, A. Toga, A. Evans, M. Petrides, Three-dimensional MRI atlas of the human
25
26 498 cerebellum in proportional stereotaxic space, *Neuroimage.* 10 (1999) 233–260.
27
28 499 <https://doi.org/10.1006/nimg.1999.0459>.
29
30 500
31 501 [21] N.P.M. Todd, S. Govender, J.G. Colebatch, Vestibular cerebellar evoked potentials in
32
33 502 humans and their modulation during optokinetic stimulation, *J. Neurophysiol.* 120 (2018)
34
35 503 3099–3109. <https://doi.org/10.1152/jn.00502.2018>.
36
37 504
38 505 [22] N. Jeyakumar, S. Govender, J.G. Colebatch, Properties of short-latency responses in the
39
40 506 upper limbs evoked by axial impulses during leaning: evidence for reticulospinal projections,
41
42 507 *Exp. Brain. Res.* 236 (2018) 2611-2618. <https://doi.org/10.1007/s00221-018-5320-5>.
43
44 508
45 509 [23] L.M. Nashner, P. Wolfson, Influence of head position and proprioceptive cues on short
46
47 510 latency postural reflexes evoked by galvanic stimulation of the human labyrinth, *Brain. Res.*
48
49 511 67 (1974) 255-268. [https://doi.org/10.1016/0006-8993\(74\)90276-5](https://doi.org/10.1016/0006-8993(74)90276-5).
50
51 512
52
53 513 [24] F.B. Horak, H.C. Diener, Cerebellar control of postural scaling and central set in stance,
54
55 514 *J. Neurophysiol.* 72 (1994) 479-493. <https://doi.org/10.1152/jn.1994.72.2.479>.
56
57 515
58 516 [25] D. Timmann, F.B. Horak, Prediction and set-dependent scaling of early postural
59
60 517 responses in cerebellar patients, *Brain* 120 (1997) 327-337.
61
62
63
64
65

518 <https://doi.org/10.1093/brain/120.2.327>.
1
2 519
3
4 520 [26] C. Asanuma, W.T. Thach, E.G. Jones, Brainstem and spinal projections of deep
5 521 cerebellar nuclei in the monkey, with observations on the brainstem projections of the dorsal
6 522 column nuclei, *Brain. Res. Rev.* 286 (1983) 299-322.
7
8
9 523 [https://doi.org/10.1016/0165-0173\(83\)90017-6](https://doi.org/10.1016/0165-0173(83)90017-6).
10
11 524
12
13 525 [27] X.Y. Zhang, J.J. Wang, J.N. Zhu, Cerebellar fastigial nucleus: from anatomic
14 526 construction to physiological functions, *Cerebellum Ataxias* 3 (2016) 3:9.
15
16 527 <https://doi.org/10.1186/s40673-016-0047-1>.
17
18 528
19
20 529 [28] J.C. Eccles, R.A. Nicoll, D.W.F. Schwarz, H. Taborikova, T.J. Willey, Reticulospinal
21 530 neurons with and without monosynaptic inputs from cerebellar nuclei, *J. Neurophysiol.* 38
22 531 (1975) 513-530. <https://doi.org/10.1152/jn.1975.38.3.513>.
23
24
25 532
26
27 533 [29] T.C. Watson, N. Becker, R. Apps, M.W. Jones, Back to front: cerebellar connections and
28 534 interactions with the prefrontal cortex, *Front. Syst. Neurosci.* 4 (2014) 8:4.
29
30 535 <https://doi.org/10.3389/fnsys.2014.00004>.
31
32 536
33
34 537 [30] A. Brodal, *Neurological Anatomy in Relation to Clinical Medicine*. Oxford University
35 538 Press, New York, 1981.
36
37
38 539
39
40 540 [31] J.G. Colebatch, S. Govender, D.L. Dennis, Postural responses to anterior and posterior
41 541 perturbations applied to the upper trunk of standing human subjects, *Exp. Brain. Res.* 234
42 542 (2016) 367-376. <https://doi.org/10.1007/s00221-015-4442-2>.
43
44
45 543
46
47 544
48
49 545
50
51 546
52
53 547
54
55 548
56
57 549
58 550
59
60 551
61
62
63
64
65

552

1
2 553

3
4
5
6
7
8
9
10
11
12
13
14
15
16
17
18
19
20
21
22
23
24
25
26
27
28
29
30
31
32
33
34
35
36
37
38
39
40
41
42
43
44
45
46
47
48
49
50
51
52
53
54
55
56
57
58
59
60
61
62
63
64
65

554

1
2
3
4
5
6
7
8
9
10
11
12
13
14
15
16
17
18
19
20
21
22
23
24
25
26
27
28
29
30
31
32
33
34
35
36
37
38
39
40
41
42
43
44
45
46
47
48
49
50
51
52
53
54
55
56
57
58
59
60
61
62
63
64
65

FIGURE CAPTIONS

556

Figure 1. (A) CEP grand means for the axial (C7) stimuli averaged across timing conditions. The scalp potential map demonstrates a series of short latency waveforms, centered around Iz. Over the cerebellar electrodes, potentials consisted of a series of waves (P13/N19/P25/N32/P50/N62). Over the frontal electrodes, longer latency N1/P2/N2 waves can be observed which are largest at FCz. (B) Potential maps demonstrate the dipole orientated in the midline over the cerebellar electrodes. For illustrative purposes, only a subset of the 63 electrodes is shown. *The AFz waveform reflects the average of recordings from the AF3 and AF4 locations.

565

Figure 2. (A) CEP grand means for the vestibular stimulus applied to the left side of the head, averaged across timing conditions. The scalp potential map demonstrates a short latency biphasic waveform contralateral to the side of stimulation which is largest over PO10 (P12/N17). Additional short latency peaks (N25/P40/N53) can also be seen at Bz. Similar to axial stimulation, long latency N1/P2/N2 waves were observed frontally. (B) In contrast to axial stimulation, potential maps show the dipole strongly lateralised for vestibular stimulation. For illustrative purposes, only a subset of the 63 electrodes is shown. *The AFz waveform reflects the average of recordings from the AF3 and AF4 locations.

574

Figure 3. The global field power (GFP) and grand means at FCz and Iz for the axial stimulus (A) and GFP and grand means at FCz and PO10 for the vestibular stimulus (B). Sequences of short and long latency lobes can be seen for both stimuli. The dashed vertical line demarcates the start of the long latency epoch, as defined for source analysis.

579

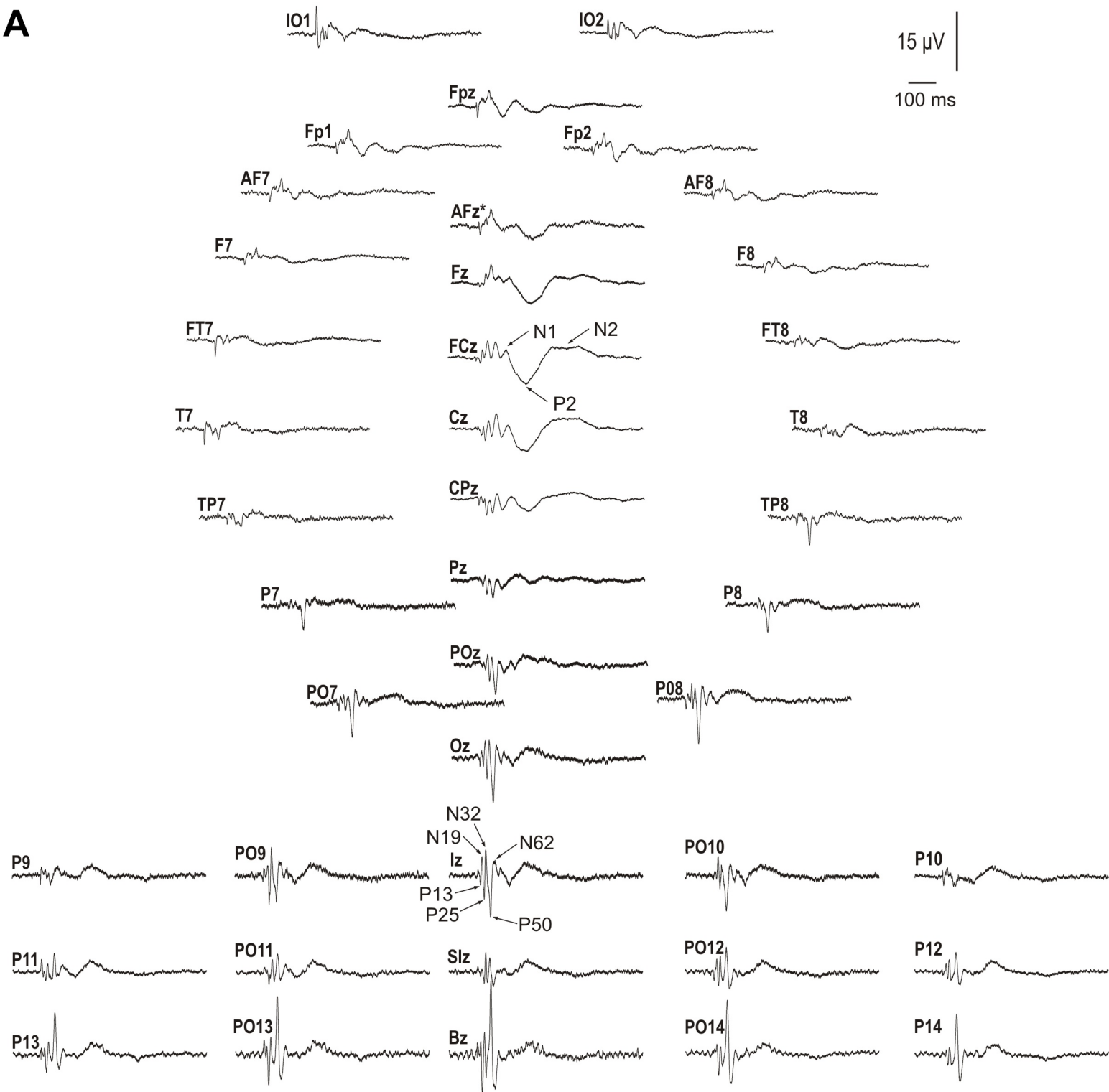
Figure 4. BESA source analysis result (4-dipole solutions). Cerebellar and fronto-central locations rendered in an average MRI (A, C) and the corresponding source currents (B, D) for axial (left column) and vestibular (right column) stimulation. In both cases, sources 1 and 2 (Sc1, Sc2) were in the midline frontally and sources 3 and 4 (Sc3, Sc4) lay in the cerebellum.

584

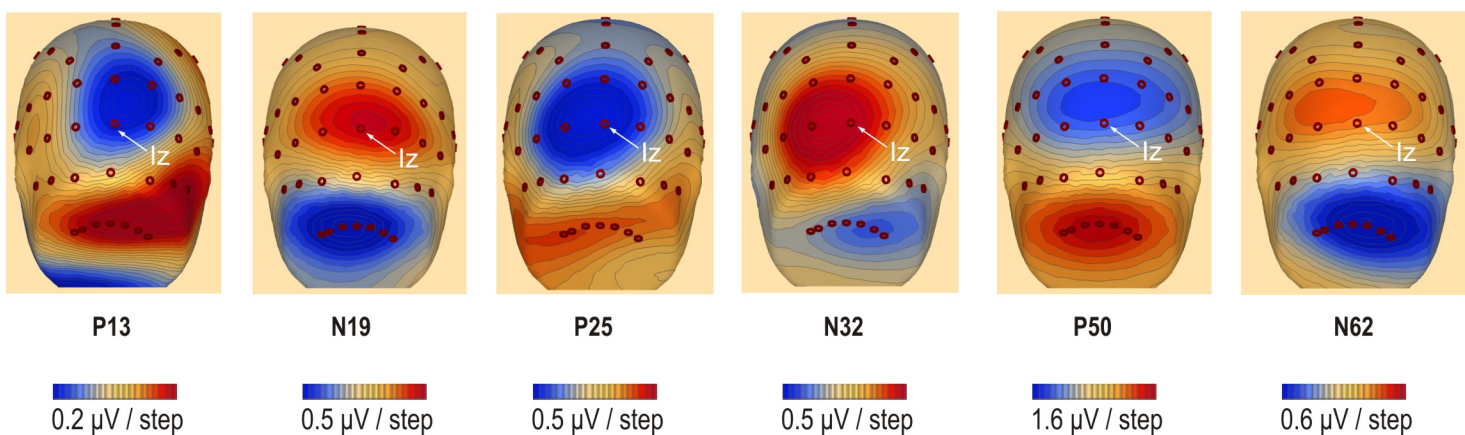
Figure 5. Scaleograms (parts A & G) showing the changes in spontaneous cerebellar activity for axial and vestibular stimulation using only the irregular condition. Note pause-burst (B) and burst-pause (H) post-stimulus changes in the very (VHF) and ultra-high frequency (UHF)

588 bands. Source currents for the two cerebellar sources using the 4 source models (C & I)
1 589 correspond with those of the neural evoked responses at Iz (D) and PO10 (J), in particular the
2
3 590 larger P12 vestibular and P50 axial waves. RMS EMG recordings showed SL responses in
4
5 591 the soleus (SOL) muscles for both modalities which consisted of an excitation-inhibition for
6
7 592 axial stimulation (E) and inhibition-excitation for vestibular stimulation (K). For both
8
9 593 modalities, SL EMG responses occurred about 45 ms after the onset of the neural response
10
11 594 (see text). Responses in tibialis anterior (TA) were either negligible or consisted of cross-talk
12
13 595 from the larger soleus response. Note that the tonic level of EMG has been removed (soleus
14
15 596 mean 125 μ V, TA mean 36.5 μ V). Accelerometry traces from over the tibia (F & L) showed
16
17 597 larger induced accelerations for the axial stimulus. The darker traces in E and K show the
18
19 598 RMS averages, the lighter the unrectified ones. $mg = 10^{-3} g$
20
21
22
23
24
25
26
27
28
29
30
31
32
33
34
35
36
37
38
39
40
41
42
43
44
45
46
47
48
49
50
51
52
53
54
55
56
57
58
59
60
61
62
63
64
65

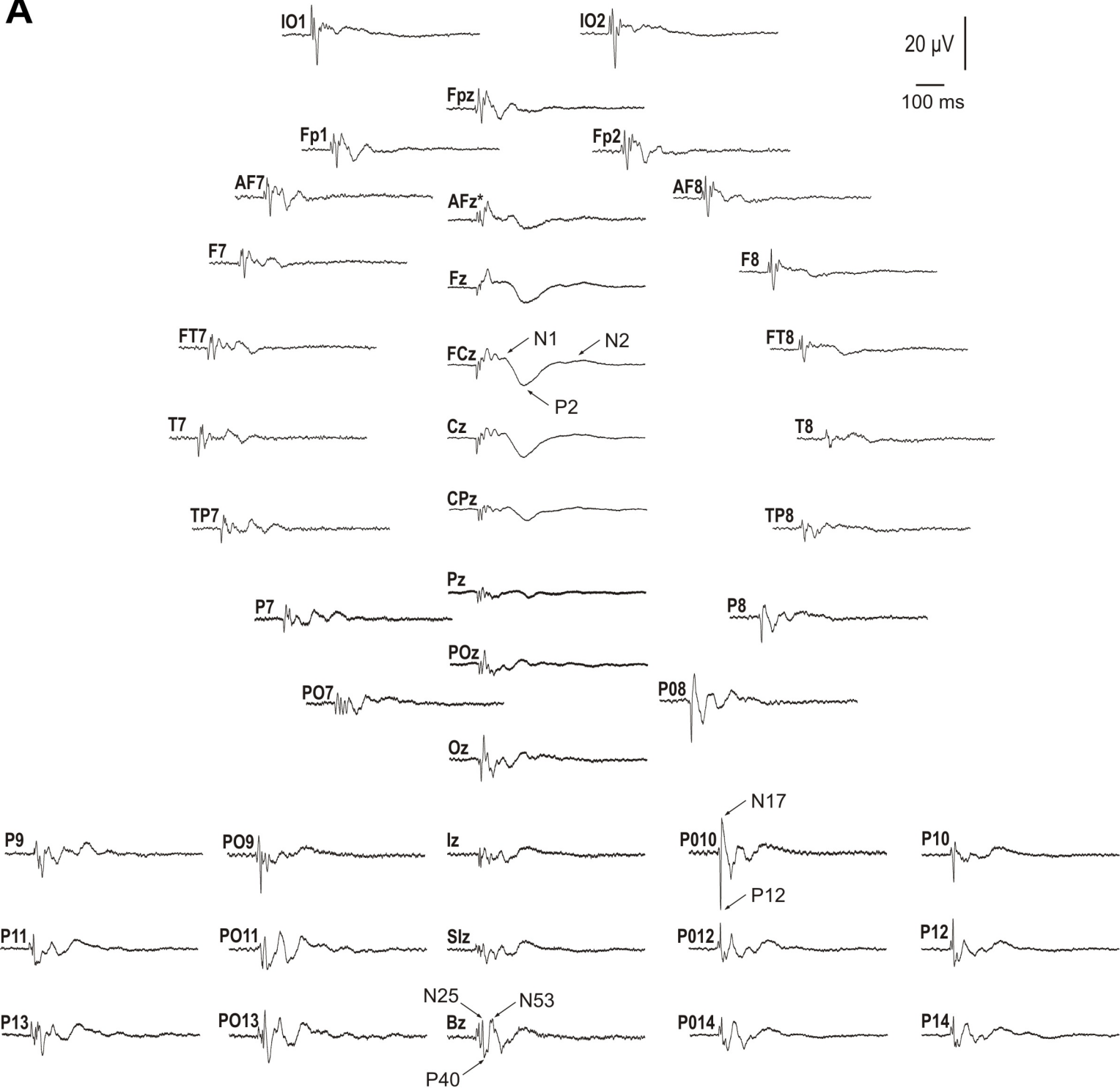
A



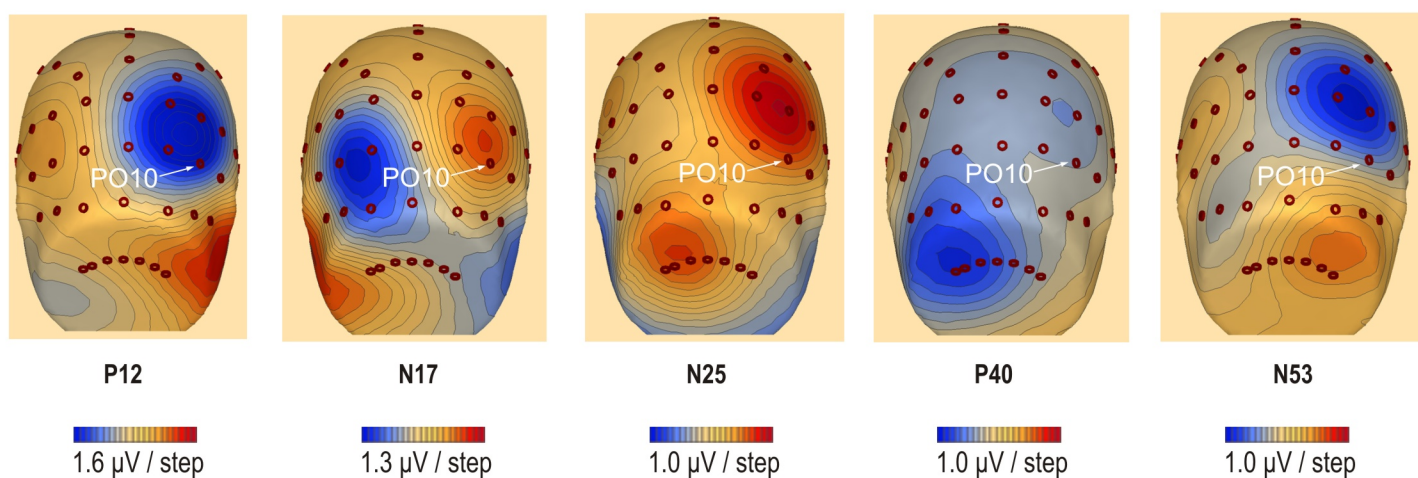
B

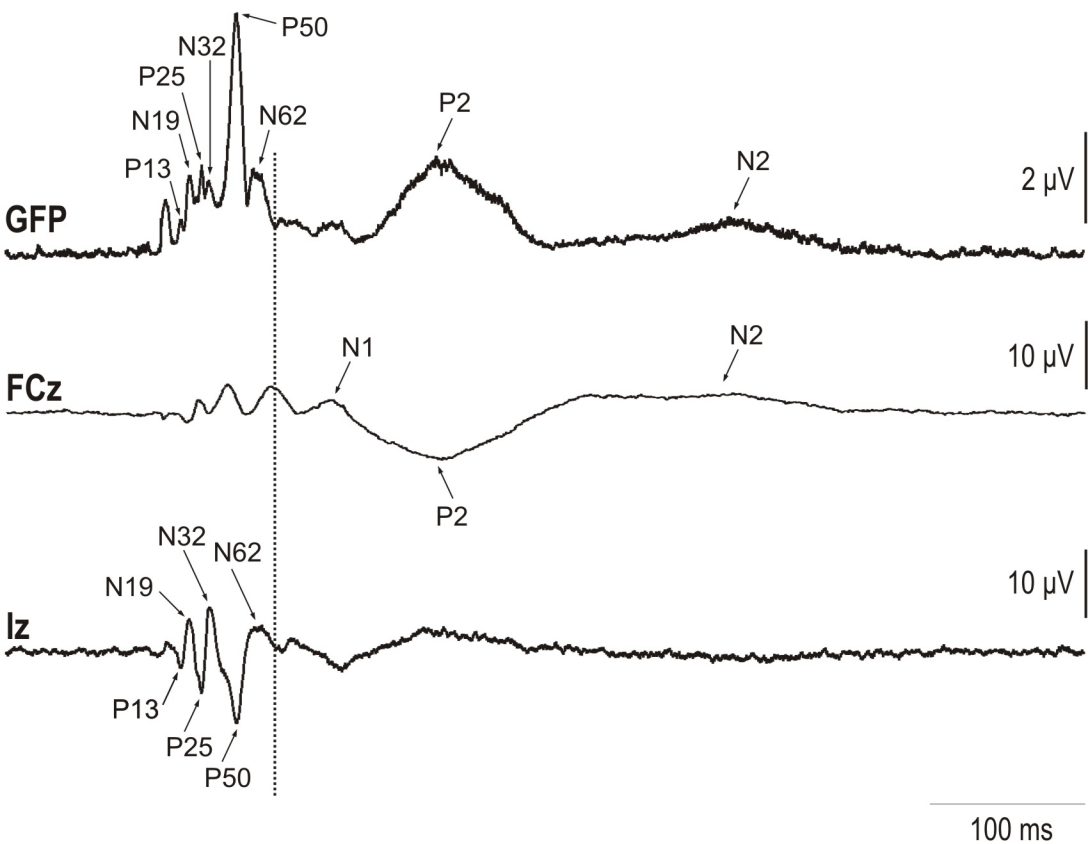


A

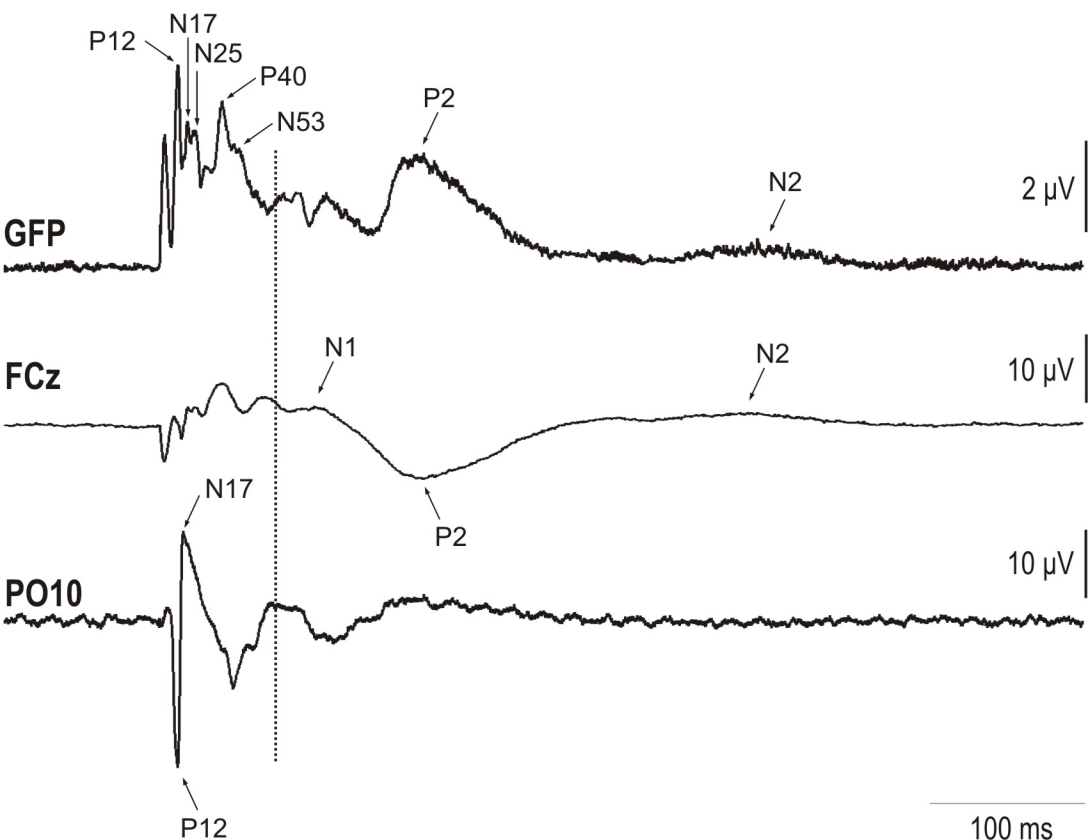


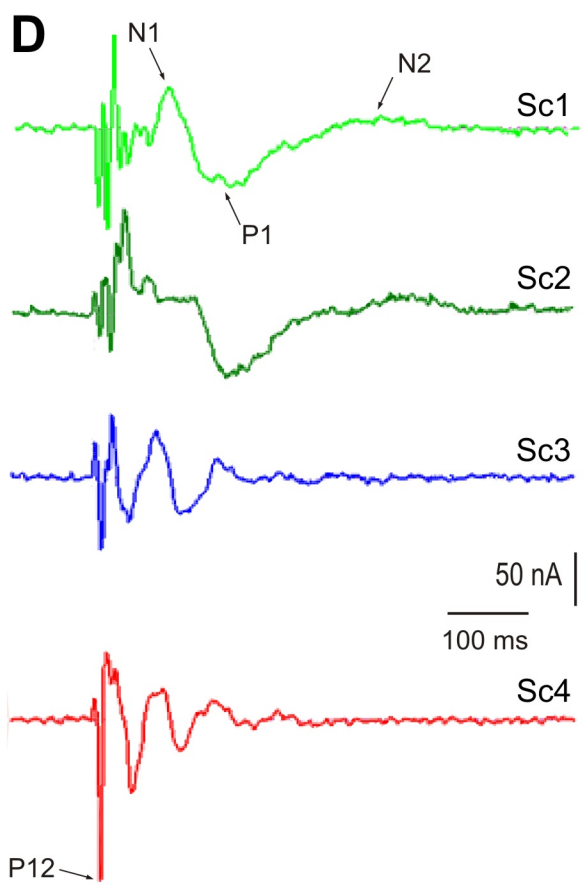
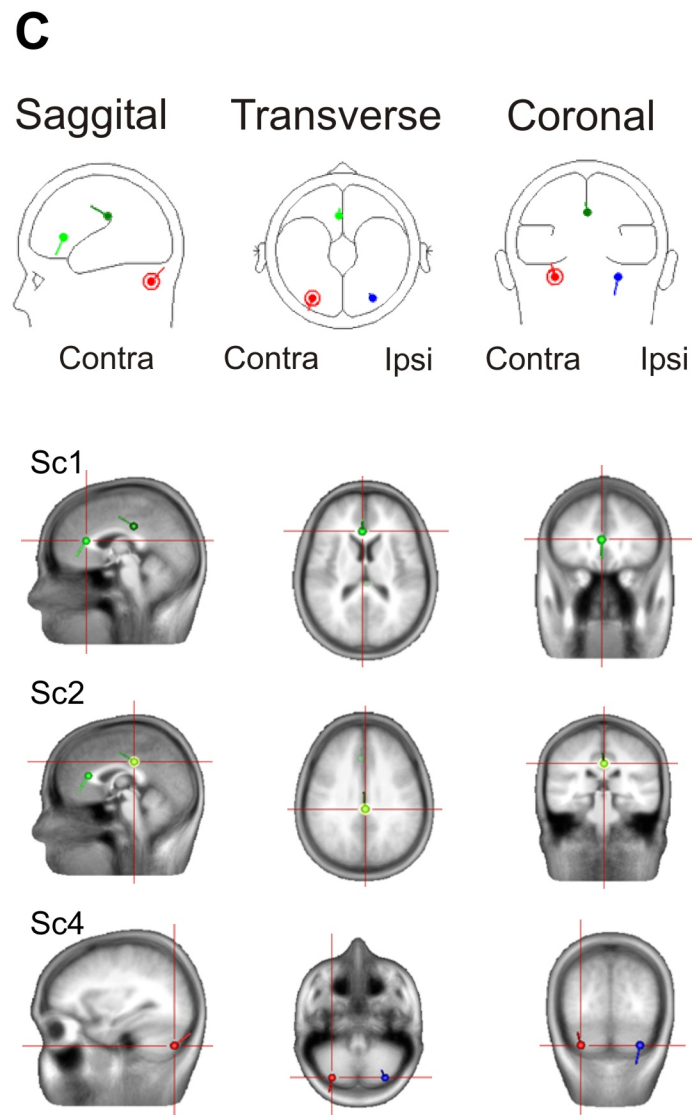
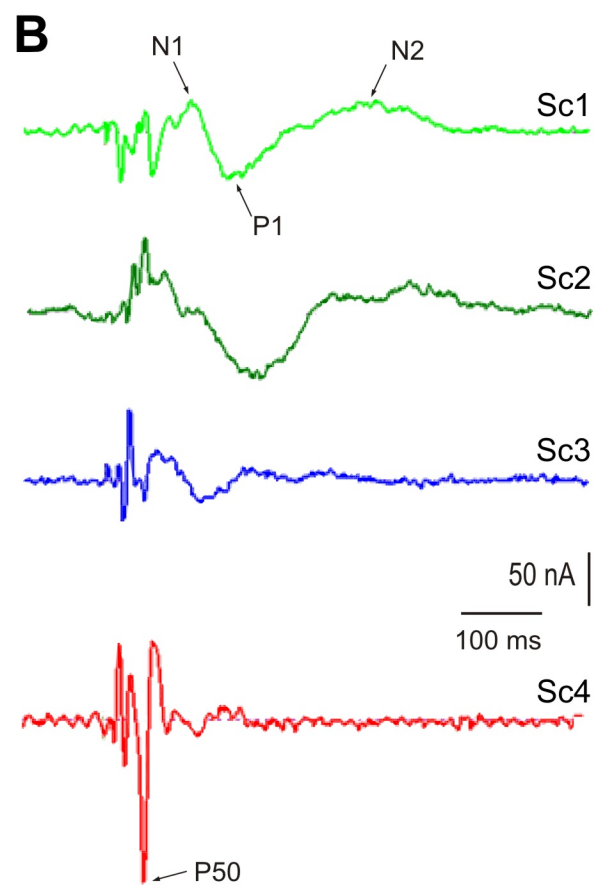
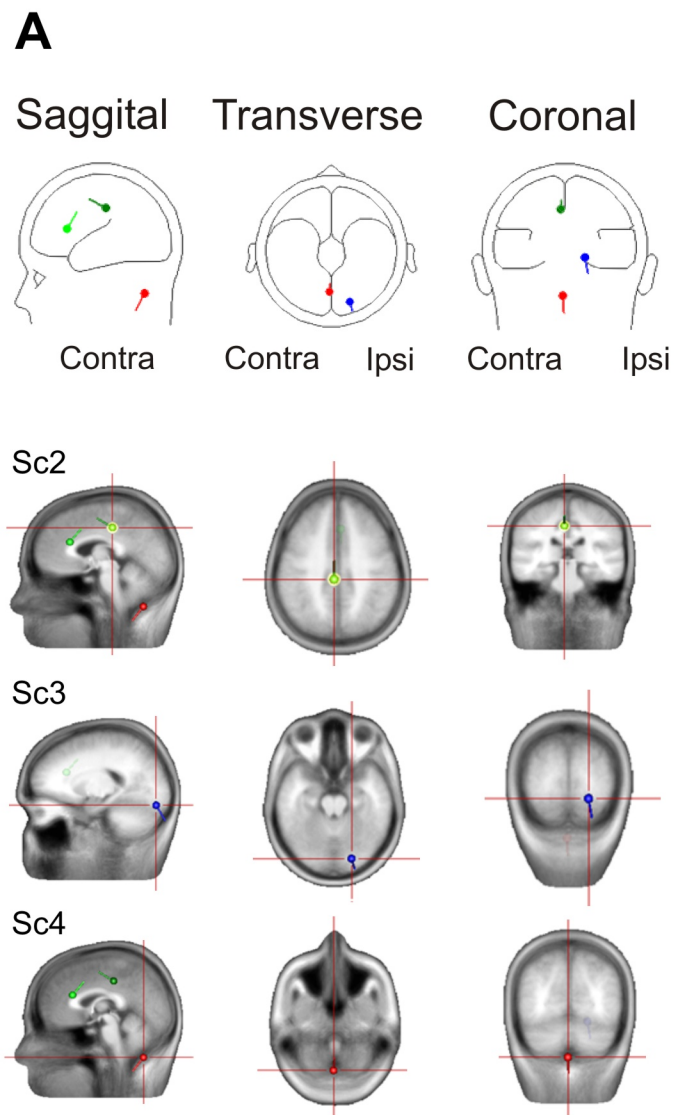
B





B Vestibular stimulation





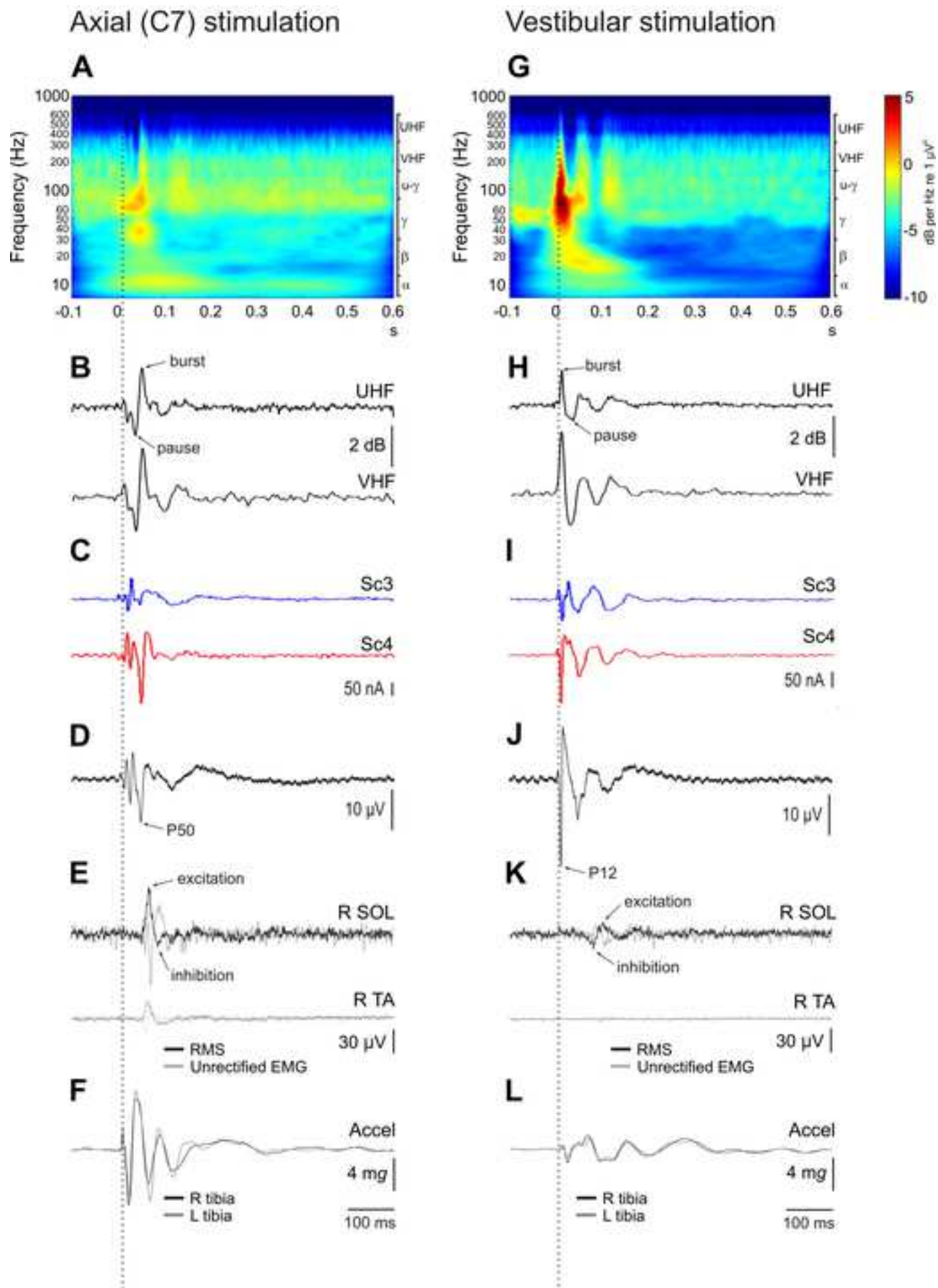


TABLE I: Axial and vestibular short and long latency potential latencies (ms) and amplitudes (μV)

AXIAL	P13	N19	N1	P2	N2
Amplitude					
Irregular	11.3 (6.2)	15.0 (2.7)	10.9 (6.1)	16.9 (6.2)	12.4 (4.5)
Regular	7.9 (11.4)	11.3 (8.1)	5.7 (10.6)	15.5 (4.4)	13.1(4.3)
Uncertain (beat present)	9.2 (10.4)	13.9 (7.9)	10.1 (6.2)	16.7 (6.0)	11.1 (4.3)
Uncertain (beat absent)	11.5 (5.9)	13.8 (8.3)	12.8 (5.6)	17.4 (6.7)	11.2 (4.8)
Mean (SD)	9.8 (8.4)	13.5 (6.7)	9.9 (7.3)	16.6 (5.4)	11.9 (4.2)
Latency					
Irregular	13.5 (1.0)	19.1 (3.1)	108.4 (8.1)	178.0 (17.0)	287.4 (32.7)
Regular	13.1 (2.2)	18.4 (2.3)	104.6 (11.1)	174.2 (9.8)	291.0 (34.7)
Uncertain (beat present)	13.0 (2.1)	18.8 (2.0)	106.6 (8.2)	185.8 (17.6)	299.2 (23.6)
Uncertain (beat absent)	12.4 (2.8)	18.8 (1.9)	106.6 (8.4)	181.4 (12.4)	294.6 (12.4)
Mean (SD)	12.8 (2.2)	18.8 (2.2)	106.9 (8.4)	179.8 (14.0)	293.1 (28.0)
VESTIBULAR	P12	N17	N1	P2	N2
Amplitude					
Irregular	26.3 (8.6)	21.8 (10.8)	14.6 (4.6)	18.6 (5.5)	9.4 (8.4)
Regular	28.3 (2.2)	22.4 (11.3)	8.3 (5.2)	15.0 (6.8)	2.4 (8.8)
Uncertain (beat present)	27.1 (4.4)	23.2 (7.1)	12.2 (2.4)	18.1 (5.1)	5.3 (5.4)
Uncertain (beat absent)	28.1 (3.6)	21.2 (11.9)	8.6 (3.8)	18.9 (4.5)	6.9 (6.8)
Mean (SD)	27.4 (5.8)	22.3 (9.8)	10.9 (4.7)	17.6 (5.3)	6.0 (7.4)
Latency					
Irregular	12.1 (1.4)	16.8 (2.1)	104.4 (7.1)	184.2 (19.1)	295.8 (24.3)
Regular	12.1 (0.9)	16.7 (2.8)	107.6 (10.3)	161.8 (7.8)	290.0 (14.4)
Uncertain (beat present)	12.5 (1.4)	16.9 (1.7)	106.4 (11.2)	189.2 (20.0)	286.4 (18.6)
Uncertain (beat absent)	12.4 (1.3)	17.8 (3.3)	109.2 (12.7)	176.0 (22.1)	298.2 (19.5)
Mean (SD)	12.3 (1.2)	17.0 (2.4)	106.9 (9.8)	177.8 (19.7)	292.6 (18.6)

Averaged values for all subjects, for all conditions. P13, N19 peaks were recorded at Iz for axial stimulation and P12, N17 peaks were recorded at PO10 for vestibular stimulation. N1, P2 and N2 peaks were recorded at FCz.

TABLE II: ANOVA effects for axial and vestibular short and long latency potentials

	Factor	df	Amplitude		Latency	
			F	p	F	p
Short	MOD	1,4	17.7	<.05	1.5	ns
	COND	3,12	0.3	ns	0.2	ns
	WAVE	1,4	0.1	ns	124	<.001
	MOD*COND	3,12	0.8	ns	0.9	ns
	MOD*WAV	1,4	11.7	<.05	2.4	ns
	COND*WAV	3,12	0.7	ns	2.1	ns
	M*C*W	3,12	0.3	ns	0.2	ns
Long	MOD	1,4	0.5	ns	0.1	ns
	COND	3,12	5.3	<.05	2.7	ns
	WAVE	2,8	9.9	<.05	359	<.001
	MOD*COND	3,12	2.2	ns	0.5	ns
	MOD*WAV	2,8	3.9	ns	0.0	ns
	COND*WAV	6,24	1.0	ns	1.9	ns
	M*C*W	6,24	2.1	ns	1.5	ns

Abbreviations: MOD, M – stimulus modality; COND, C – condition; WAV, W – wave, ns- not significant. The latency findings simply confirm the different wave latencies.

TABLE III: Summary of BESA results: axial stimulation, 10-dipole model.

Location	Side	Epoch	Brain Area	Weight	X	Y	Z
CEREBRAL CORTEX							
Frontal cortex							
ACG	R	w	24,32	0.8	6	30	14(Sc1)
	L	w	24,32,33	0.2	-10	21	17
ReG, MeFG, SuCaG, OrG	L	s	11,25	0.6	-6	21	-19
MeFG, IFG, SuCaG	L	w	25,47,11,10	0.7	-10	27	-14
CG, MeFG	R	s	24,6,31	0.9	5	-3	44
MeFG, Mi FG	L	w,s	6	0.2	-14,17	-15	54,56
Fronto-parietal cortex							
PoCeG, PrCeG	L	s	6,3,4	0.3	-41	-17	64
	R	w	3,4	0.3	26	-27	56
PC L, CG, MeFG, PCun	L+R	w	31,5,6,7	1.5	1	-27	46(Sc2)
Temporal cortex							
ITG, MTG	L	s	20,38	0.2	-38	-1	-51
FG, PHG	L	w	37,36	0.6	-43	-37	-7
MTG, STG	R	w	39,22	0.3	48	-51	6
Temporo-parietal cortex							
Insula, STG, IPL	R	w	13,41	0.2	42	-39	18
Parietal cortex							
PCG	L	w	23,30,29	0.4	-9	-57	16
Parieto-occipital cortex							
Cun, PCG	R	s	30,31,18,23	0.2	12	-65	11
Occipital cortex							
MOcG	R	s	18,19	0.3	33	-89	7
SUBCORTEX							
Brainstem							
Pons	L+R	w		0.4	0	-33	-15
Medulla	L	s		0.4	-8	-38	-55
Cerebellum							
Lobule IX (tonsil)	L	s		0.3	-9	-50	-56
	L+R	s,w		1.1,1.0	-1,2	-58,59	-57(Sc4)
Lobule V	L	s		0.9	-4	-76	-15
Lobule VIIB	L	w		0.2	-28	-81	-54(Sc3)
Crus II	L	w		0.7	-11	-82	-39
Crus II, lobule VIIB	L	s		0.6	-34	-85	-43
Lobule VIIB, crus II	R	s		1.0	31	-85	-52
Crus II	R	w		0.8	25	-86	-37
Neck							
Neck	R	s		0.3	15	-94	-49
	L	w		0.5	-21	-100	-22
	L	s		0.3	-28	-101	-26

Abbreviations: Anterior cingulate gyrus (ACG), cingulate gyrus (CG), cuneus (Cun), inferior frontal gyrus (IFG), inferior parietal lobule (IPL), inferior temporal gyrus (ITG), insula (Ins), fusiform gyrus (FG), medial frontal gyrus (MeFG), middle frontal gyrus (MiFG), middle occipital gyrus (MOcG), middle temporal gyrus (MTG), orbital gyrus (OrG), paracentral lobule (PCL), parahippocampal gyrus (PHG), postcentral gyrus (PoCeG), posterior cingulate gyrus (PCG), precentral gyrus (PrCeG), precuneus (PCun), subcallosal gyrus (SuCaG).

TABLE IV: Summary of BESA results: vestibular stimulation, 10-dipole model.

Location	Side	Epoch	Brain Area	Weight	X	Y	Z
CEREBRAL CORTEX							
Frontal cortex							
ACG	L+R	w	24	0.9	0	24	3(Sc1)
CG	R	s	32,24	0.3	6	14	33
	R	s	24	0.3	6	-1	39
	L+R	s	24,23	0.6	-1	-10	25(Sc2)
	L	w	24,33,31	0.2	-6	-18	37
	R+L	w	31,24,23	0.7	4	-24	37
Me FG, Mi FG, CG,PCL	R	s	6,24,31	0.2	18	-8	52
CG,PCL	L	s	24,31	0.4	-4	-13	40
SUBCORTEX							
Eyes							
Eyes	L+R	w		0.9	-7	71	-33
Basal Ganglia							
Caudate	R	w		0.2	9	17	6
Thalamus							
MDN,Pulv, LDN, VLN	L	w		0.3	9	-20	16
Brainstem							
Pons (within 9mm)	R	s		0.9	6	2	-28
Medulla	R	w		0.8	5	-38	-55
Cerebellum							
Lobule IX (tonsil)	L	s		0.9	-3	-54	-57
Lobule VIIIA	L	s		0.9	-37	-42	-56
Lobule VIIIB	L	w,s		0.6,0.2	-32,27	-46,52	-56(Sc3)
	L	s,w		0.2,0.3	-15,21	-62,64	-58
Lobule VIIIA/VIIB	L	w		0.4	-27	-71	-49
	R	w		0.7	31	-72	-53(Sc4)
	R	s		0.7	32	-72	-52
Lobule VIIB	L	w		0.7	-36	-74	-58
	L	s		0.7	-38	-73	-58
	L	s		0.9	-28	-82	-47
Crus I/ II	L	w		0.2	-47	-74	-37
Crus I	L	w		0.3	-37	-86	-37
Neck							
Neck	R	w,s		0.9,1.0	26,24	-97,98	-41,38

Abbreviations: Anterior cingulate gyrus (ACG), cingulate gyrus (CG), lateral dorsal nucleus (LDN), medial dorsal nucleus (MDN), medial frontal gyrus (MeFG), middle frontal gyrus (MiFG), pulvinar (Pulv), paracentral lobule (PCL), ventral lateral nucleus (VLN).

Credit Author Statement

All authors contributed significantly to the design of the experiment. Data capture and analysis was primarily conducted by NPT and SG. Drafting of the manuscript was conducted by all authors. Revision of the manuscript was conducted primarily by JC and SG, with inputs from NPT.